Supplementary Material

Direct electrochemistry of glucose oxidase immobilized on ZrO_2 nanoparticles-decorated reduced graphene oxide sheets for a glucose biosensor

A.T. Ezhil Vilian[a], Shen-Ming Chen[a*] , M. Ajmal Ali [b], Fahad M.A. Al-Hemaid[b]

[a]Department of Chemical Engineering and Biotechnology, National Taipei University of Technology, No.1, Section 3, Chung-Hsiao East Road , Taipei 106, Taiwan (R.O.C).

[b]Department of Botany and Microbiology, College of Science, King Saud University, Riyadh 11451, Saudi Arabia.

Footnotes

* Corresponding authors. **Shen-Ming Chen,** Fax: +886 2270 25238; Tel: +886 2270 17147; E-mail: smchen78@ms15.hinet.net.

1. Atomic Force Microscopy (AFM) and Raman spectra analysis

Fig. S1 presents the AFM images of GO (A), ZrO_2 (B) and RGO-ZrO_2 composite (C). AFM image of GO shows the typical sheet like morphology of GO sheets with sheets thickness about 1 to 2 nm. AFM image of ZrO_2 presents the particle like morphology revealing the formation of ZrO_2 particles with particle size ranging in micrometers. AFM image of RGO-ZrO_2 shows the uniform decoration of ZrO_2 particles on the RGO sheets revealed the successful formation of RGO-ZrO_2 composite.

Fig. S2 shows the Raman spectra of GO (a), ZrO_2 (b) and RGO-ZrO_2 composite (c). Raman spectrum of GO (curve a) shows the D (arises from defect mediated zone- edge phonons, near K-point), G (due to doubly degenerate E_{2g} mode at the Brillouin zone cetre) and 2D (second order of zone-boundary phonons) bands at 1350 cm^{-1}, 1589 cm^{-1} and 2730 cm^{-1} respectively. [1] Similarly, ZrO_2 also presents these three bands in its Raman spectrum (curve b). It is well known that reduction of GO to RGO cause to shift these bands towards lower wavenumber and also enhance the ratio of the bands intensity. Evidently, compared the spectrum of RGO-ZrO_2 with GO, D, G and 2D bands were shifted to 1271 cm^{-1}, 1568 cm^{-1} and 2691 cm^{-1} indicated the successful reduction of GO to RGO. In addition the band intensity also greatly enhanced revealed the ample reduction GO to RGO. [2]

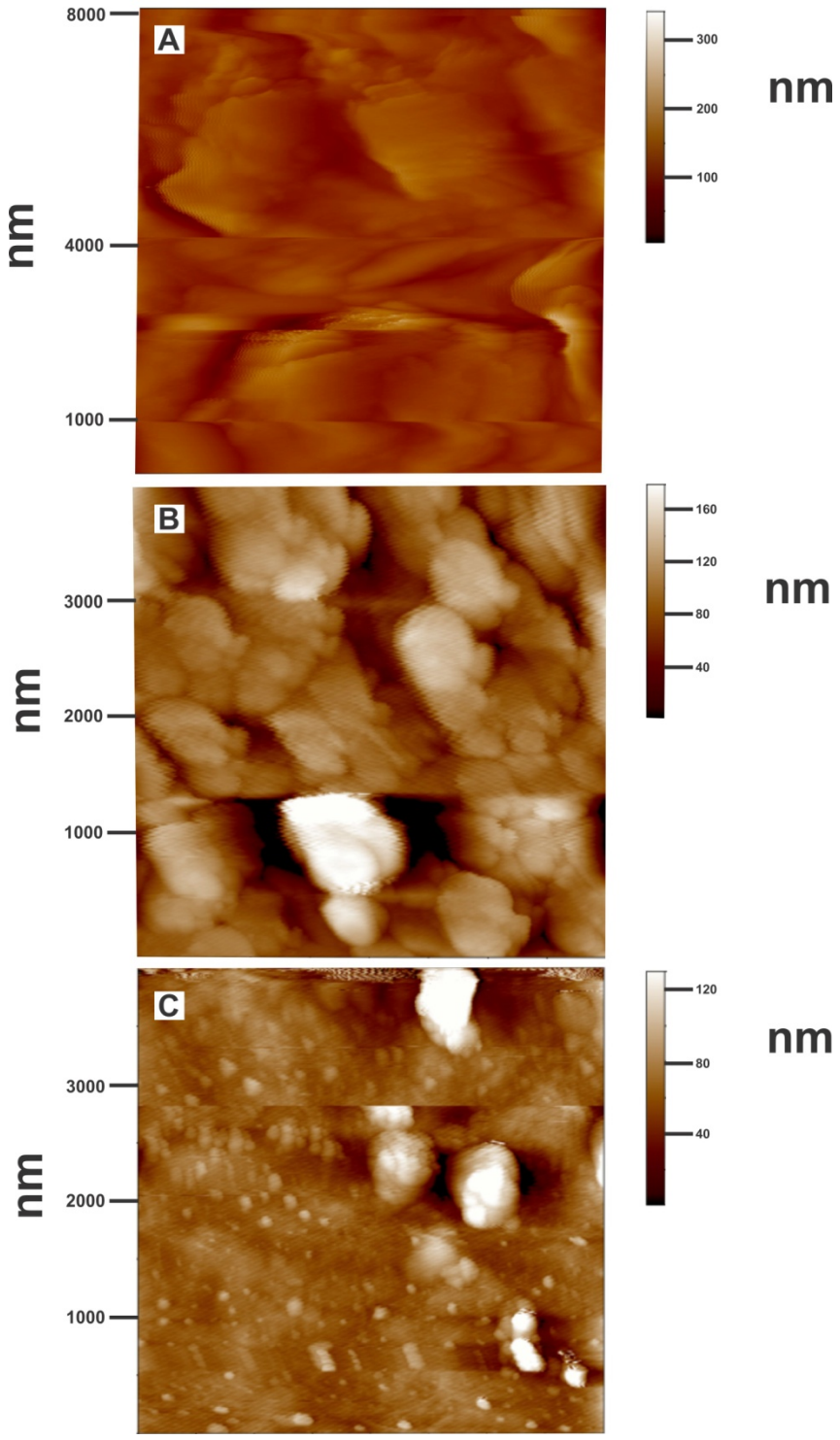

Fig. S1 AFM images of GO (A), ZrO_2 (B) and RGO-ZrO_2 (C).

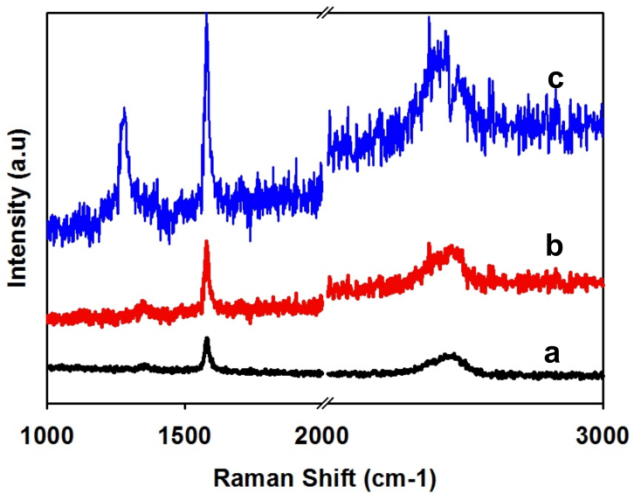

Fig. S2 Raman spectra of GO (a), ZrO_2 (b) and RGO-ZrO_2 (c).

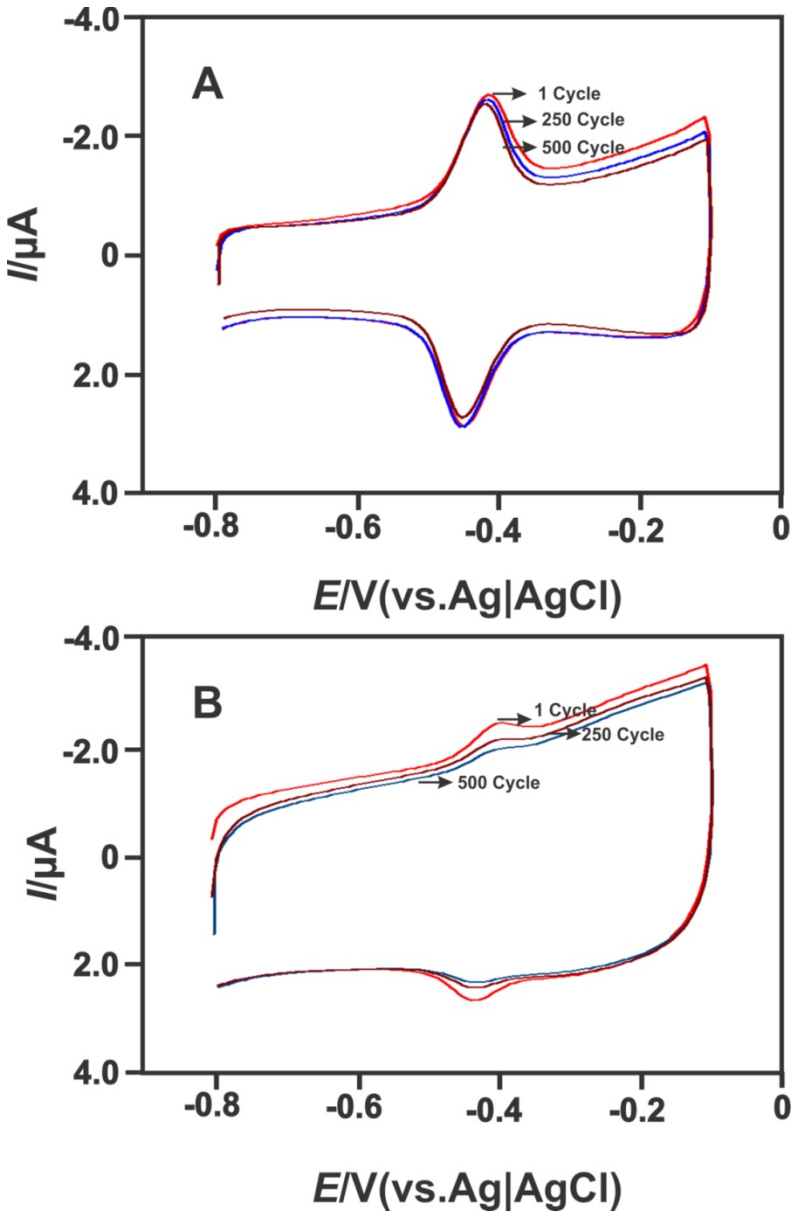

Fig. S3 Continuous CV cycles (1, 250 and 500 cycles) of GOx-PLL/RGO-ZrO_2 (a) and GOx/RGO-ZrO_2 (b) film modified GCEs in nitrogen-saturated PBS (pH 7) at the scan rate of 50 mV/s.

2. Investigation of direct electrochemistry of GOx

To investigate the individual role of RGO and ZrO_2 towards direct electrochemistry of GOx, CVs were carried out in PBS (pH 7) at the scan rate 50 mV/s (Fig. S4). Feeble redox peaks were observed at the GOx-PLL/ZrO_2 (curve a) attributed to the poor immobilization of GOx when ZrO_2 alone used as the electrode matrix. A pair of redox peaks with formal potential ($E^{o'}$) of -0.422 V responsible for the direct electrochemistry of GOx were observed at GOx-PLL/RGO/GCE (curve b). Well defined and sharp redox peaks with formal potential ($E^{o'}$) of -0.416 V were observed at GOx-PLL/RGO-ZrO_2/GCE (curve c). Peak currents were significantly increased upon combination of both RGO and ZrO_2 shows that they together assist more enzymes loading than when they were alone.

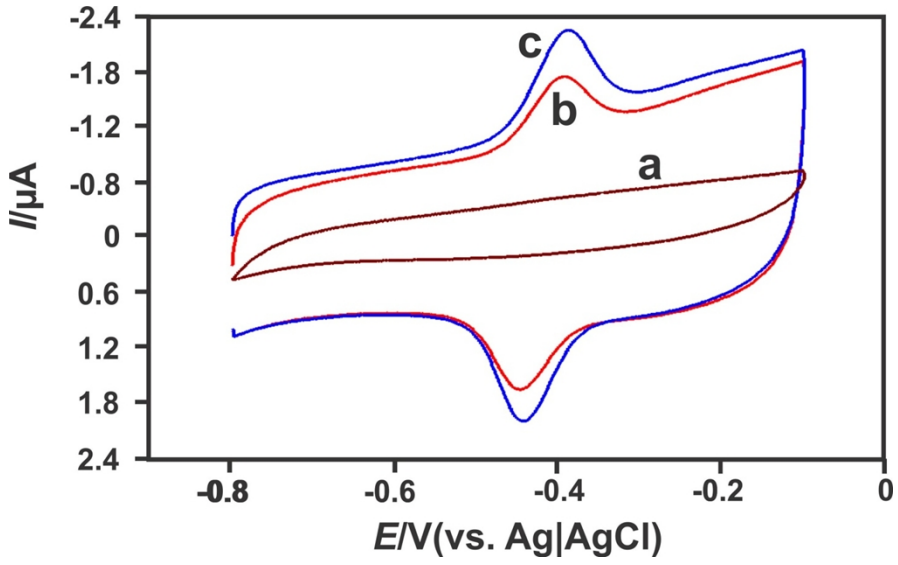

Fig. S4 CVs of GOx-PLL/ZrO_2 (a), GOx-PLL/RGO (b) and GOx-PLL/RGO-ZrO_2 (c) film modified GCEs in nitrogen-saturated PBS (pH 7) at the scan rate of 50 mV/s.

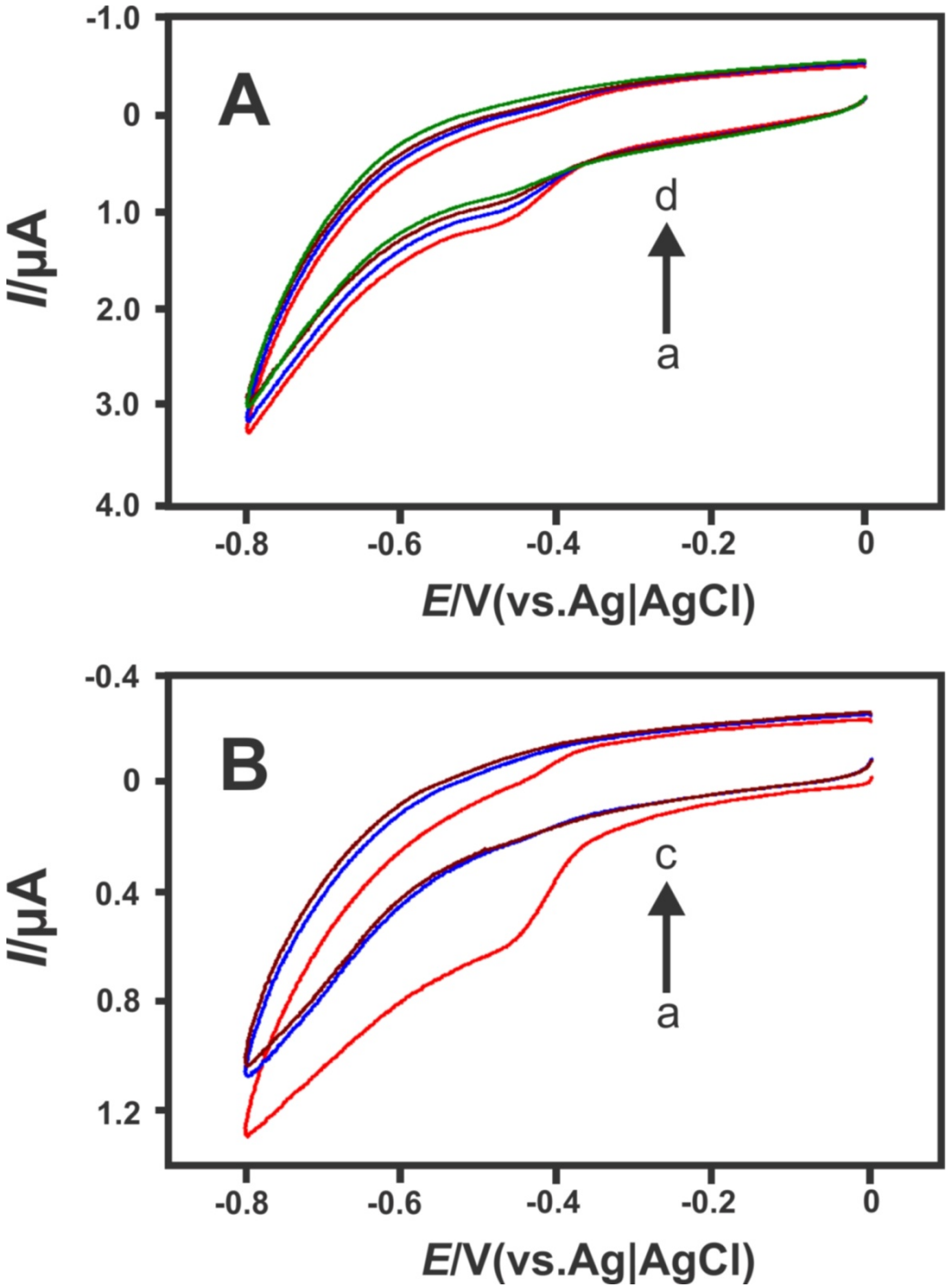

Fig. S5(A) CVs of GOx-PLL/RGO modified GCEs in oxygen saturated PBS (pH 7) containing various concentrations of glucose 0 (a), 1 (b), 2(c), and 3 mM (d) at the scan rate 50 mV s^{-1}. (B)

CVs of GOx-PLL/ ZrO_2 modified GCEs in oxygen saturated PBS (pH 7) containing various concentrations of glucose 0 (a), 1 (b), and 2(c), at the scan rate 50 mV s^{-1}

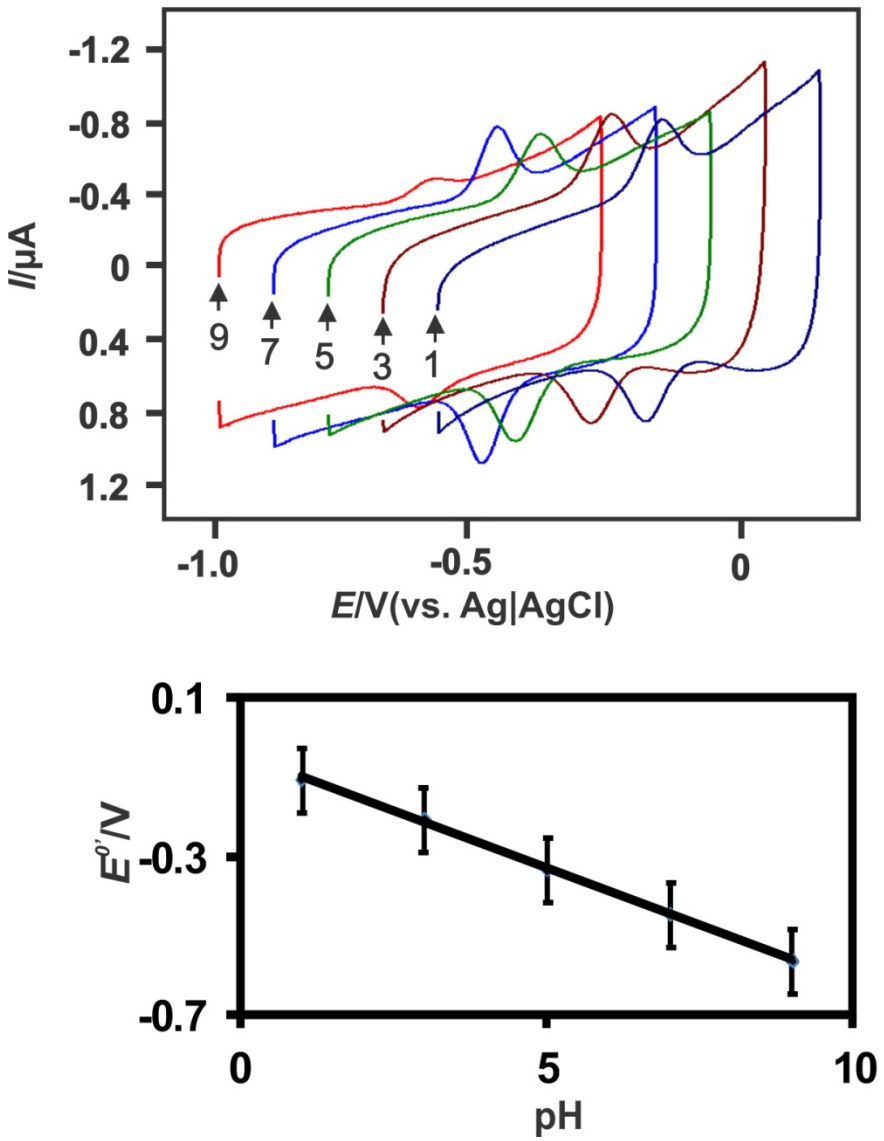

Fig. S6 (A) CVs of GOx-PLL/RGO-ZrO_2/GCE in PBS with different pH values (1 to 9). (B) Plot of $E^{o'}$ versus pH values, $E^{o'}$/V is presented as function of pH values, $E^{o'}$/V = -0.0414 (± 0.51)/V – 0.0578 (± 0.40) pH/ (V/pH), R^2 = 0.998. Error bars represent standard deviation of 3 independent measurements.

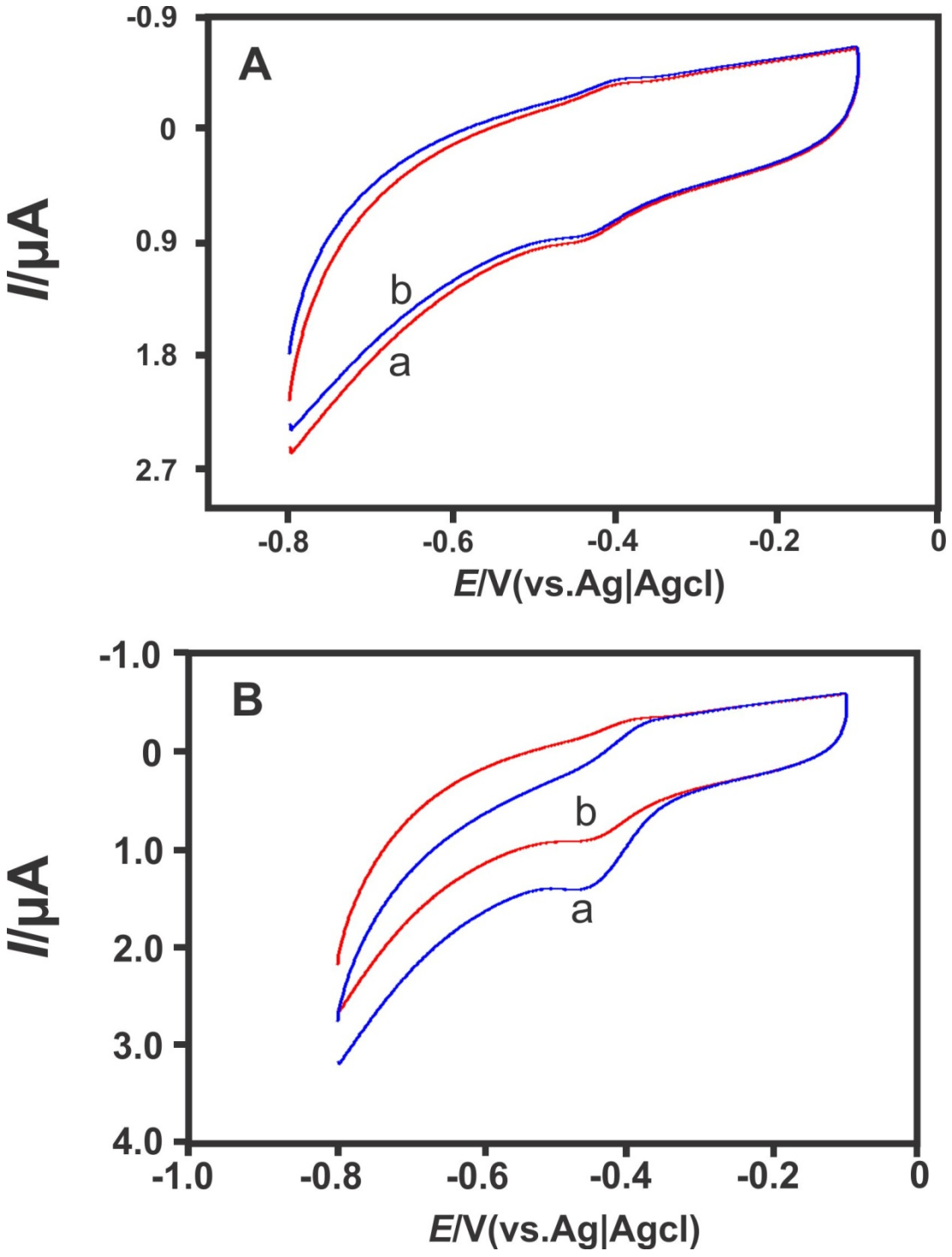

Fig. S7 CVs obtained at the GOx/RGO-ZrO_2/GCE (A) and GOx-PLL/RGO-ZrO_2/GCE (B) in the absence (a) and presence of 3 mM glucose (b) in PBS (pH 7) at the scan rate of 50 mV s^{-1}.

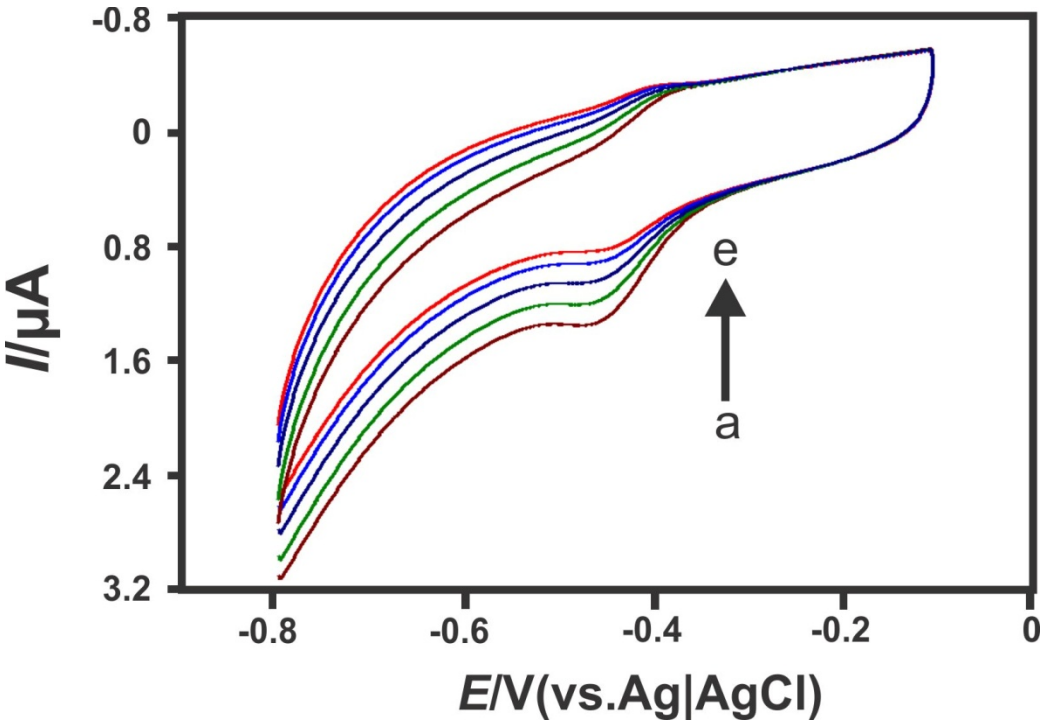

Fig. S8 CVs obtained at the GOx-PLL/RGO-ZrO_2/GCE in the absence (a) and presence of 1 mM (b), 2 mM (c), 3 mM (d) and 4 mM glucose (e) in urine samples (0.1 M PBS: human urine samples (1: 100) at the scan rate 50 mV s^{-1}.

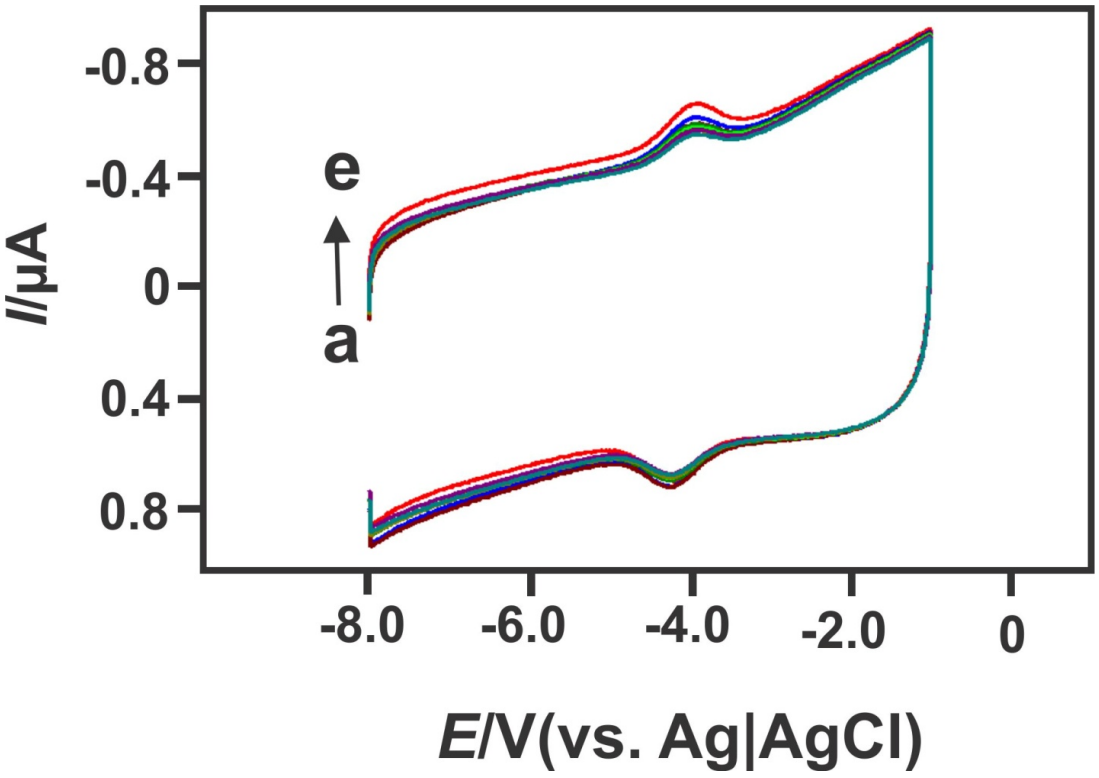

Fig. S9 Repeatability studies of the GOx-PLL/RGO-ZrO_2/GCE modified electrode in presence of 1mM glucose in PBS pH 7 (a-e, successive measurements) at the scan rate of 50 mV s^{-1}.

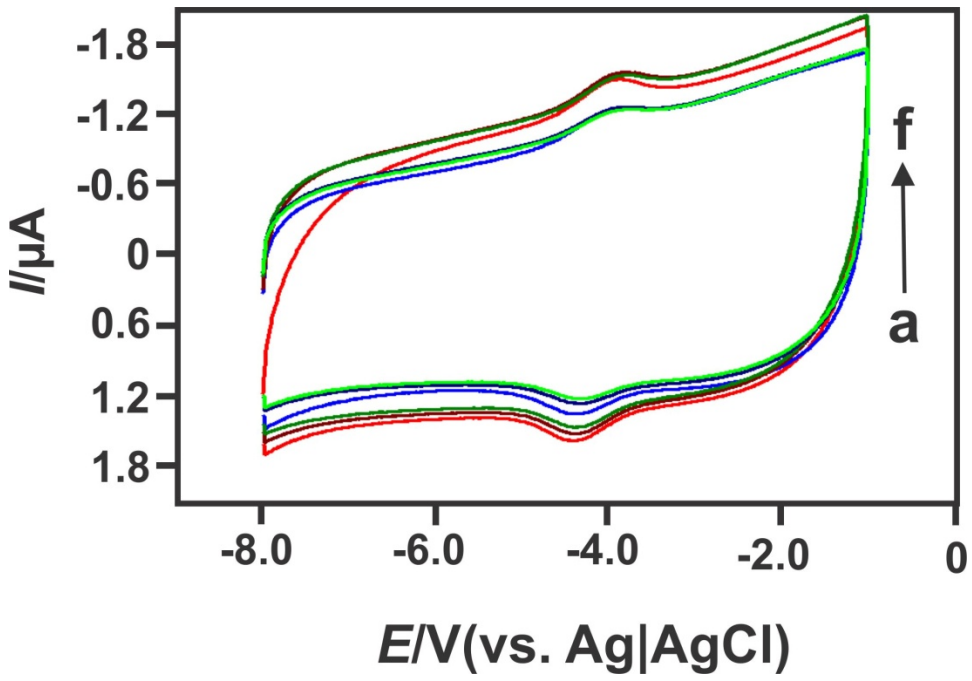

Fig. S10 Repeatability studies of the GOx-PLL/RGO-ZrO_2/GCE modified electrode (six independently) modified electrode in the presence of 1 mM glucose in PBS (pH 7) at the scan rate of 50 mV s^{-1}.

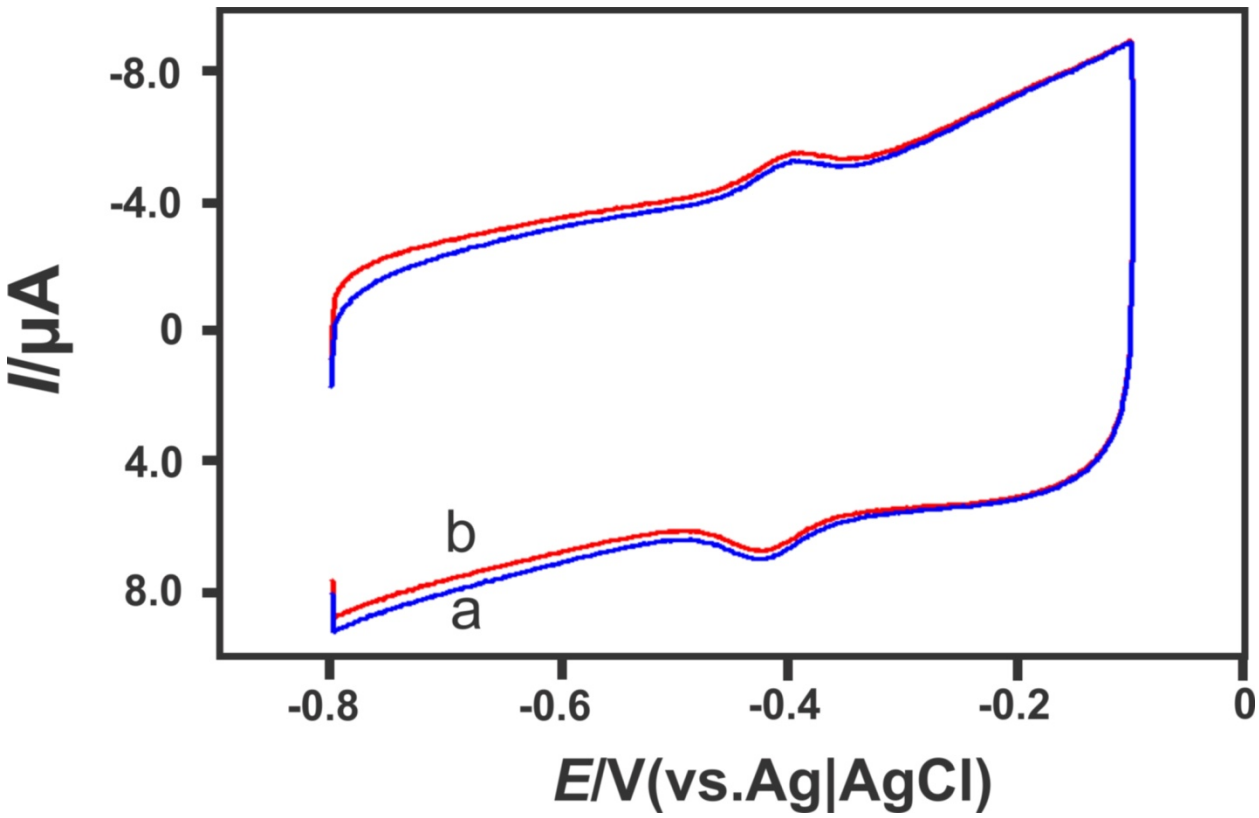

Fig. S11. Recorded cyclic voltammograms of the fresh GOx-PLL/RGO-ZrO_2/GCE modified electrode (a) and after it kept at refrigerator for 1 month (b), electrolyte was PBS pH 7 and scan rate was 50 mV s^{-1}.

Table 2

Determination of glucose in spiked human urine samples at GOx-PLL/RGO-ZrO_2/GCE

Samples	Added/mM	Found/mM	Recovery/%
1	2.0	1.94	97
2	3.0	2.96	98.66
3	4.0	4.11	102.75

References

1. C. Ferrari, J.C. Meyer, V. Scardaci, C. Casiraghi, M. Lazzeri, F. Mauri, S. Piscanec, D. Jiang, K.S. Novoselov, S. Roth, A.K. Geim, *Phys. Rev. Lett*. 2006, **97,**18740(1-4).
2. R. S. Dey, C. R. Raj, *J. Phys. Chem. C*, 2010, **114**, 21427-21433.